Species-specific oculomotor control tolerances predict saccadic suppression strength in macaques and zebrafish

Giulia Soto[1,#], Florian A. Dehmelt[1,#], Matthias P. Baumann[1,2,#], Ibrahim Tunç[1,2,3,4], Yue Yu[1,2], Tatiana Malevich[1,2], Ziad M. Hafed[1,2]*, Aristides B. Arrenberg[1,*]

[1] Werner Reichardt Centre for Integrative Neuroscience, University of Tübingen, Tübingen, Germany
[2] Hertie Institute for Clinical Brain Research, University of Tübingen, Tübingen, Germany
[3] Graduate Training Centre of Neuroscience, University of Tübingen, Tübingen, Germany
[4] Current address: Computational Systems Neuroscience, Institute of Zoology, University of Cologne, Cologne, Germany
* corresponding authors: aristides.arrenberg@uni-tuebingen.de, and ziad.m.hafed@cin.uni-tuebingen.de
[#] contributed equally

Summary

Active sensing necessarily requires integrating information about both self-generated movements as well as past, present, and future afferent inputs[1,2]. However, such information is inherently variable and relies, at least in part, on uncertain extrapolations. Here, using saccadic suppression[3,4] of visual sensitivity as a classic example of sensory-motor integration, we show that suppression strength in two drastically different species, macaque monkeys and zebrafish larvae, may be a direct outcome of efficient state estimation in the presence of uncontrollable sensory and motor variability. Bayesian estimator models[5] suggest that optimal saccadic suppression should rely not just on the sensory-motor information being processed, but also on the time-dependent magnitude of unexplained variability in the nervous system encoding it. In both macaques and zebrafish larvae, and using matched visual stimulation regimes across the species, we experimentally measured saccadic suppression strength in the superior colliculus (SC) of the monkeys and the homologous optic tectum (OT) of the fish. We also experimentally quantified additive and multiplicative noise components in the motor systems of both species, and we furthermore estimated noise in the sensory systems. We found that inter-species differences in noise levels and their theoretically predicted impacts on visual sensitivity are qualitatively consistent with our experimentally observed differences in saccadic suppression strength between the fish and the monkeys. Because sensory and motor noise levels can reflect the amounts of available neural resources committed to a given task, our results strongly underscore the value of incorporating computational resource limits in investigating performance differences that have evolved in homologous brain areas.

Results and Discussion

When moving through the world, our brains constantly reconcile potentially conflicting information arising from sensory inputs in a changing environment and from the internal signals of our own body movements. One striking example of this non-stationary relationship between sensory and motor information is the active vision phenomenon of saccadic suppression: a brief reduction in visual sensitivity around the time of saccadic eye movements[3,4,6–10] (Figure 1A).

Saccadic suppression is a highly conserved phenomenon across a wide range of species, from zebrafish larvae[11] to rodents[9,10] and primates/humans[3,4,7,9,12,13]. However, the neural resources in these different species are very drastically different (e.g. Figures 1B-C), providing us with an ideal opportunity to understand how computational limits in different brain sizes act to quantitatively reshape what are otherwise qualitatively identical phenomena in multiple species.

Starting from a theoretical foundation, we implemented a computational model allowing parameterization of different sensory and motor noise contributions to saccadic suppression strength. Then, using matched visual stimulation paradigms (Methods), we experimentally measured saccadic suppression strength in homologous brain structures within macaque monkeys and zebrafish larvae, two species at opposite ends of the evolutionary spectrum. Our results revealed a particularly important effect of sensory noise in dictating saccadic suppression strength in the two species.

Saccadic suppression as efficient sensory-motor estimation

Eye position control can be optimized in a closed-loop system, and a recent study suggested that saccadic suppression might be caused by efficient sensory-motor estimation across rapid eye movements[5]. According to this framework (Figure 1D), a Bayesian estimator dynamically balances predictions from both sensory and motor information according to their ever-changing reliability, particularly across saccades. Uncertainty arises explicitly from four distinct sources: the sensory input (additive sensory

noise, σ_t), the dynamics of the eye plant (additive motor noise, ξ_t), the control signal itself (multiplicative motor noise, ε_t), and the relay delay of sensory signals, δt, from the retina to higher computing areas. Taking these variable sources of noise into account, specifically around the time of rapid eye movements, sensory signals are very unreliable in estimating the eye plant's instantaneous state. Thus, to optimize state estimation during saccades, sensory signals should be discounted and motor signals preferred.

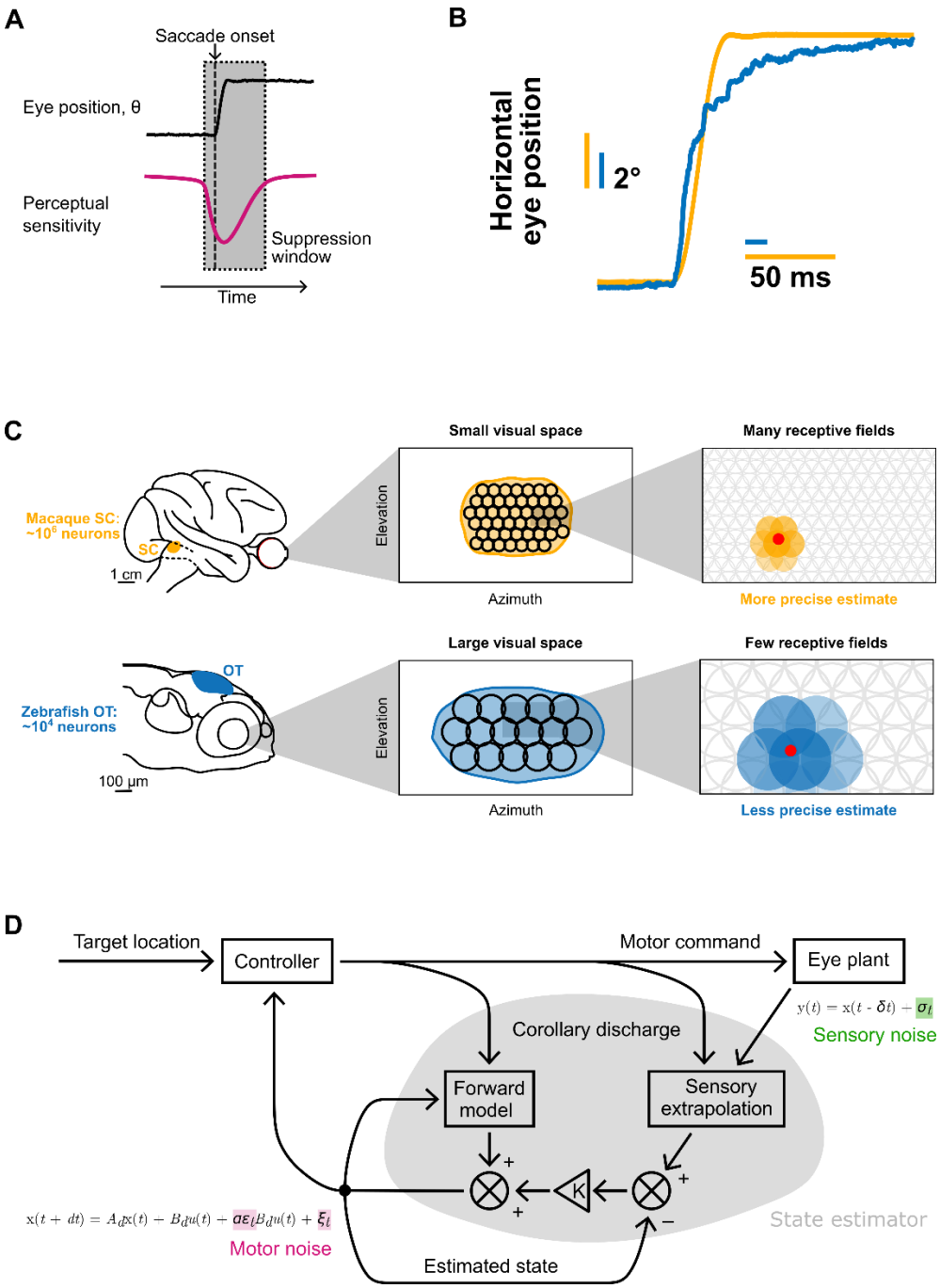

Figure 1. Saccadic suppression as efficient sensory-motor estimation.

(A) In a suppression window around the time of a saccadic eye movement, visual perception is reduced.

(B) Horizontal eye position during a saccadic eye movement of macaques (orange trace) and zebrafish (blue trace). The zebrafish saccade is executed slower and less accurately than the macaque saccade.

(C) Schematic linking neuronal resources to accuracy of sensory estimation in macaque and zebrafish. Macaque superior colliculus (SC) contains ~100 times as many neurons as the homologous zebrafish optic tectum (OT). This allows macaques to sample their significantly smaller visual field with many small-size receptive fields. Whereas zebrafish have to fill a large visual field (here centered around the area centralis) with fewer larger receptive fields. Thus, macaques can estimate the position of a visual stimulus (red dot) more precisely than zebrafish.

(D) Schematic illustration of Bayesian state estimation for closed-loop control of eye movements (adapted from Crevecoeur and Kording[5]). To estimate the current position x of a visual target, its previous position is relayed as visual input y with delay δt and visual noise σ_t, then combined with motor activity from the corollary discharge. This extrapolation with sensory information is weighted against a purely feedforward motor extrapolation via Kálmán filter K. Eye position is moved towards this estimated target by motor control signal u with multiplicative noise ε_t, additive noise ξ_t., and a scaling factor α. A_t and B_t capture the dynamics of the eye plant, t is time, dt the time step. Changes in K correspond to saccadic suppression or enhancement. See Methods for the model and notations.).

The above mechanistic explanation of saccadic suppression relies on anatomical structures that combine sensory and motor signals. In mammals, this is found in the superior colliculus (SC), and in lower vertebrates such as zebrafish, in the optic tectum (OT)[14–18] (Figure 1C). Studies in the macaque SC and zebrafish OT have shown that saccadic suppression can indeed be observed in neurons within these structures[7,11,16,19,20], despite their large evolutionary distance from one another. Having said that, while the SC and OT are anatomically homologous, they vary vastly in size, and therefore in their ability to contribute neural resources to the optimization task required by saccadic suppression. For example, we estimated, based on brain volume and the total number of neurons in each organism, that the macaque SC has ~100 times as many neurons as the zebrafish OT (Figure 1C, Methods). Concomitantly, observations of eye position during saccadic eye movements in zebrafish and macaques (Figure 1B) revealed less accurate saccadic eye movement execution in zebrafish, indicating less precise motor control. Further, when comparing sensory accuracy (Figure 1C), we noted that zebrafish have a much larger visual field compared to macaques, and with fewer neurons and larger receptive fields[21–23], this visual field is much more coarsely sampled in

zebrafish. In summary, the zebrafish oculomotor system may have to rely on much more uncertain visual and motor information than that of macaques, particularly peri-saccadically. As we show below, this has direct implications on the strength of saccadic suppression in the two species.

Zebrafish motor signals are much noisier than those of macaques during saccadic eye movements

To assess the effect of noise levels on theoretical predictions of efficient sensory estimation, we experimentally quantified motor noise before, during, and after saccades in macaque monkeys and zebrafish (Figure 2). We recorded saccade traces (see Methods, "Noise estimation") in both species (Figures 2A and C) and estimated noise parameters for use in the model (Figures 2B, 2D). First, eye traces were split into pre-saccadic, saccadic, and post-saccadic sections (Figures 2B, 2D). Pre- and post-saccadic sections were used to determine additive motor noise, ξ, since it is modeled as independent of the motor control signal for saccades (see Methods, "Additive motor noise"). This represents the instability of eye position in the absence of a motor control signal. To quantify multiplicative motor noise, ε, we fit a sigmoidal curve to the saccadic section of the eye traces (Figures 2B and D). From the time derivative of the sigmoidal fit, we derived the control signal u(t). A piecewise-constant approximation of u(t), combined with the previously determined additive motor noise, ξ, was then used to estimate ε (see Methods, "Multiplicative motor noise"). This represents the variability of the saccadic motor control signal and the resulting change of eye position. We thus determined that zebrafish motor control is much noisier than that of macaque monkeys, with the additive motor noise being about 10 times higher in zebrafish, and the multiplicative motor noise being nearly 40 times higher (Figure 2E). In our subsequent simulations, both types of motor noise were coupled, and always covaried.

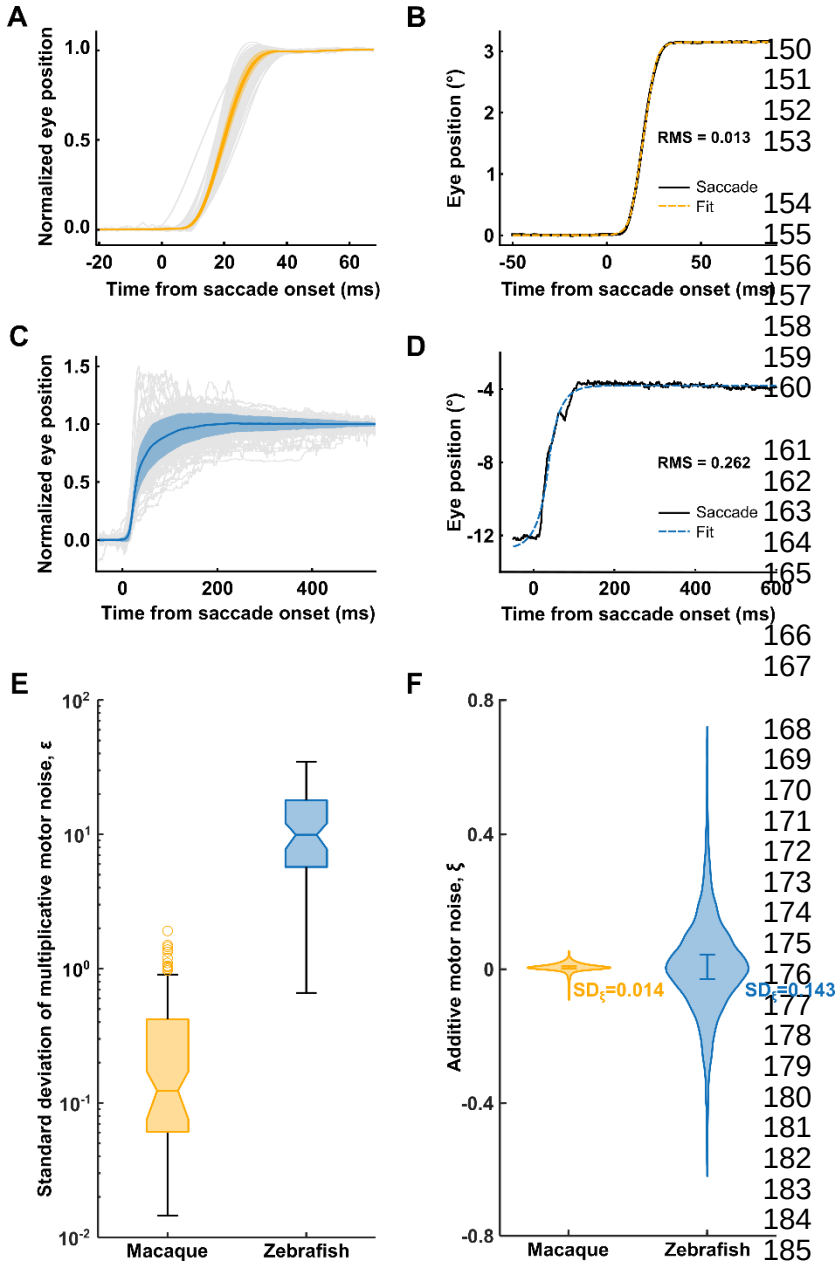

Figure 2. Zebrafish motor signals are much noisier than those of macaques during saccadic eye movements.

(A) Normalized eye position during saccadic eye movements in macaques. Grey lines indicate individual trials, colored line indicates average eye position and shaded envelope indicates standard deviation.

(B) Example macaque saccade with sigmoidal fit (dashed line). Deviations from the fit (RMS) are considered motor noise (for detailed description see STAR Methods).

(C and D) Same as (A) and (B) for zebrafish.

(E-F) Standard deviations of the estimated multiplicative (ε) motor noise, representing the saccadic motor control signal, and the estimated additive (ξ) motor noise, representing pre- and post-saccadic variability of eye positions. Boxplot shows standard deviations of multiplicative motor noise estimates for multiple velocity bins for macaque and zebrafish during saccadic eye movement (see STAR Methods). Central line indicates median, box encloses 25th to 75th percentile and whiskers extend to minimum and maximum of data; circles show outliers. (F) Violin plot shows distribution of additive motor noise estimates pooled across all pre- and post-saccadic stationary phases for macaque and zebrafish; error bars indicate the standard deviation.

On the assumption that the precision of sensory information increases with the number of available neurons for tiling visual space, the sensory noise parameter σ for both species was estimated from the number of neurons in their respective visual brain areas (see Methods, "Estimation of neuron count", "Sensory noise"). With about 1 million neurons in the SC and 10,000 neurons in OT, we expected the sensory noise to be 10 times larger

in zebrafish compared to macaques. We were now in a position to generate predictions on saccadic suppression strength across the two species.

Suppression strength differences across species are consistent with their noise levels

We first identified model parameters to reproduce the curve predicted in the original study[5]. Then, relative to this baseline, we ran further simulations in which we increased the respective noise parameters by factors of up to 37.5 times (Figure 3A). This range included the ratios observed between macaque and zebrafish noise parameters. Higher sensory noise indeed reduced the predicted optimum of saccadic suppression strength, consistent with the notion that if sensory information is always unreliable, then saccades have less effect on the trade-off involved in efficient state estimation (Figure 3B). Because absolute contributions from different noise sources vary over time, the effect of motor noise was not symmetric to that of sensory noise: Multiplicative motor noise matters only during saccade execution, accumulates over its course and may require a post-saccadic correction; but if high levels of additive motor noise make the eye position unstable, the (inevitably delayed) sensory information may be unable to provide such a correction. When set to levels observed in zebrafish, the two coupled types of motor noise noticeably affected the time course of post-saccadic corrections, predicting post-saccadic enhancement at lower noise levels only (Figure 3C; see below and Fig. 4 for what we mean by post-saccadic enhancement). In summary, if zebrafish have higher sensory and motor noise than macaque monkeys, model results predict much stronger saccadic suppression (and post-saccadic enhancement) in monkey than in fish.

To test for such cross-species differences in saccadic suppression strength, we recorded neural activity in the SC of macaque monkeys and the OT of zebrafish. The visual stimulation regime for the fish was described recently[11], and it involved saccades across textured backgrounds; here we picked one of the background textures tested in the earlier study (low spatial frequency), and we directly compared it with observations from the macaque monkey data. In such data, the monkeys generated horizontal saccades

(rightward or leftward across a coarse texture (Methods). The texture was generated similarly to the fish experiments, with the only difference being that the spatial frequency ranges were matched to the receptive field sizes expected in the monkeys (Methods); this is a similar approach to our earlier multi-species comparisons of saccadic suppression[9,10].

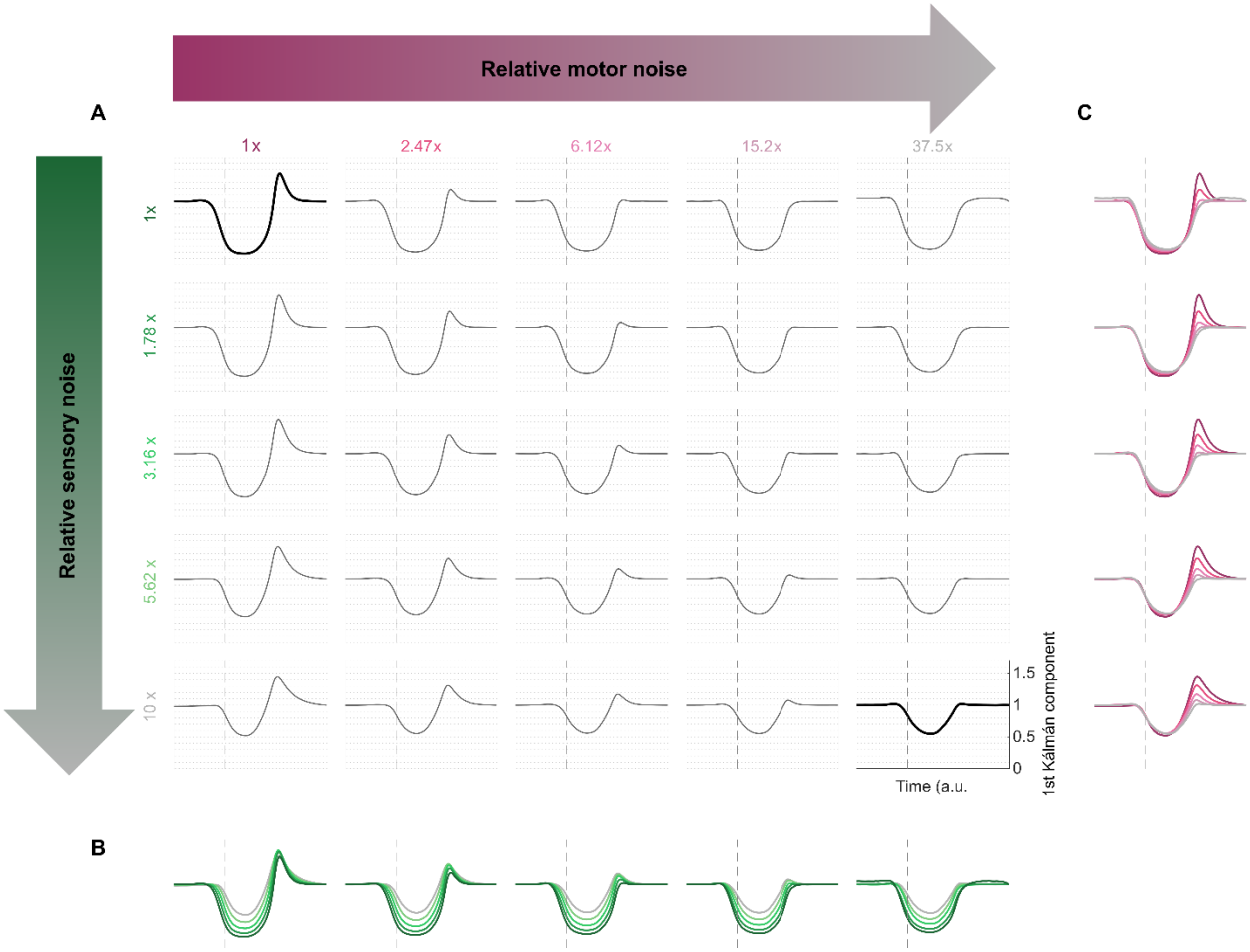

Figure 3. Bayesian model predicts differences in saccadic suppression across the range of noise parameters observed in macaque and zebrafish

(A) Optimal time course of saccadic suppression predicted by the model. All solid black traces show the first element of the optimal Kálmán matrix, vertical dashed lines show saccade onset. Different combinations of sensory and motor noise require different saccadic suppression. The thick trace on the upper left was obtained for macaque-like noise parameters, and the thick trace on the bottom right for zebrafish-like values. All noise parameters shown here (e.g., "10x") are relative to macaque values ("1x").

(B) Increased sensory noise reduces the depth of saccadic suppression across motor noise regimes, but in the parameter range investigated, hardly affects its overall shape. Curves are superpositions of those in the columns of (A), with shades of green indicating different magnitudes of sensory noise for the same motor noise.

(C) Increased motor noise discourages post-saccadic enhancement, and this effect is robust across sensory noise regimes. Curves are superpositions of those in the rows of (A), with shades of magenta indicating different magnitudes of motor noise for the same sensory noise.

Figures 4A and B schematically illustrate the timing of visual stimulus presentation relative to saccade onset in both species. Example neurons from the SC and OT are shown in Figures 4C and D, respectively. In both cases, responses to the flash were markedly reduced when the stimulus appeared shortly after a saccade, indicating clear saccadic suppression at the level of single units in both primates and fish. To compare suppression strength across the population, we computed cumulative distribution functions (CDFs) of suppression indices (Methods) for all recorded neurons (Figure 4E). The distributions revealed a clear species difference: saccadic suppression in the macaque SC was generally significantly stronger (statistical results are detailed in the legend of Fig. 4). and more prevalent than in the zebrafish OT, consistent with the model prediction (Fig. 3) that higher sensory noise in zebrafish reduces the benefit of discounting sensory input during saccades. Thus, while saccadic suppression is qualitatively similar in zebrafish[11] and macaque monkeys[7,16], the quantitative differences between the species can be easily reconciled by an optimization principle related to efficient state estimation in the presence of noise.

Finally, in both species, we experimentally tested visual sensitivity at multiple times relative to saccades (Methods). This allowed us to further compare the empirical data to the predictions of our model (Figures 4F and 4G). Specifically, for both species, the model reproduced the fact that there is always an extended time period in which visual sensitivity is reduced around saccades, regardless of suppression strength. Importantly, besides correctly predicting that saccadic suppression would be stronger in monkeys than in fish – driven solely by species-specific noise levels estimated independently (cf. Figure 2), the

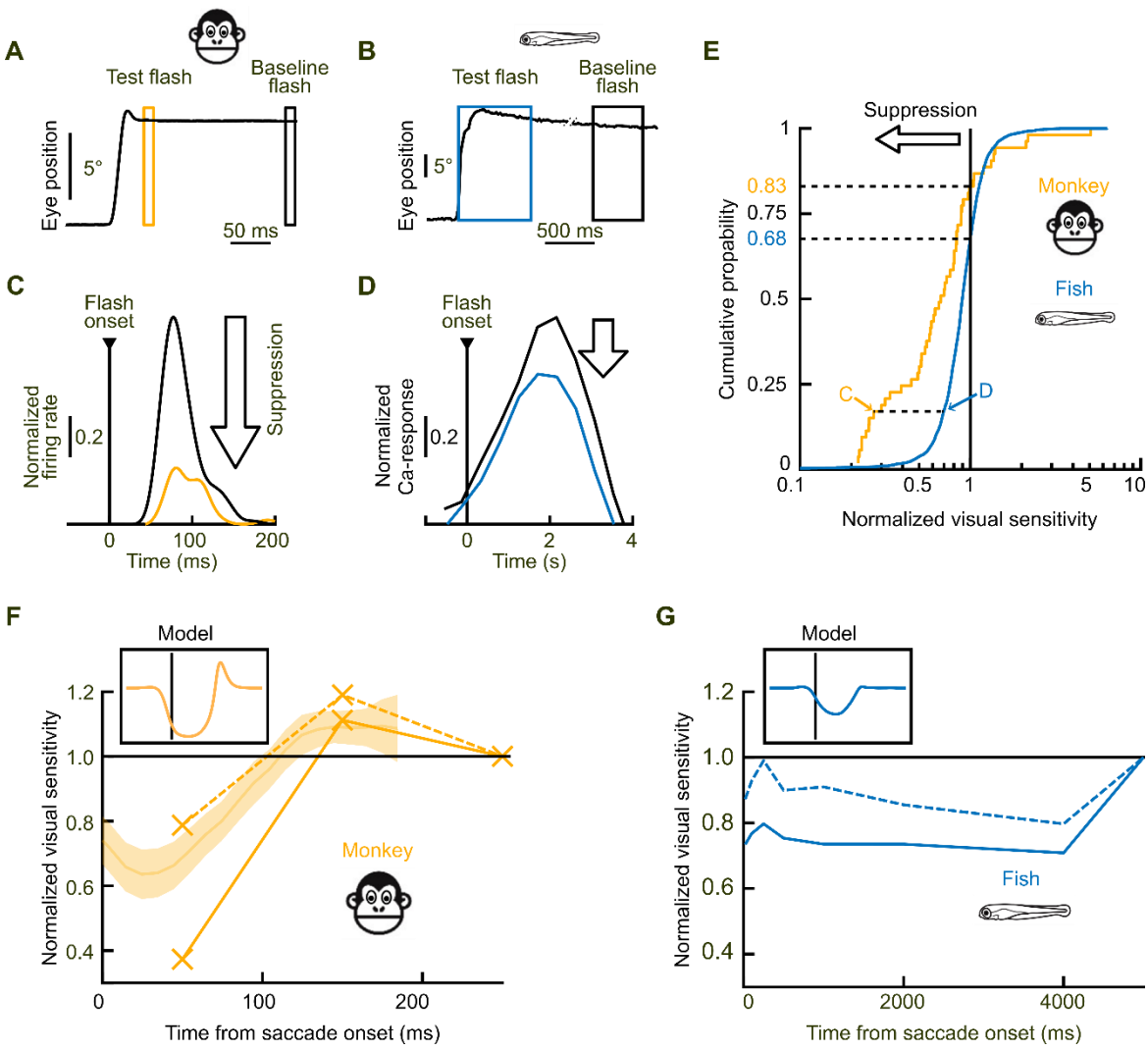

model also predicted that post-saccadic enhancement (Fig. 4F and data from Chen et al.[16]) is more likely in monkeys than in fish.

Figure 4. Saccadic suppression in the monkey superior colliculus and the zebrafish optic tectum.

(A) Example eye trace from a monkey with the timing of the baseline flash and a test flash ~50 ms after saccade onset, the saccade is highlighted in grey.

(B) Example eye movement trace from a zebrafish, illustrating baseline and test flash timing. Note: only a test flash 20 ms after saccade onset is shown here; in panels (D) and (E), test flashes at 20, 100, and 250 ms were pooled.

(C) Example neuron from monkey SC: visual response (normalized firing rate) to the baseline flash (black) and to the test flash (orange).

(D) Example neuron from zebrafish tectum: visual response (normalized calcium signal) to baseline flash (black) and pooled test flashes (blue).

(E) Cumulative distribution functions of suppression strength across neurons. Example neurons from (C) and (D) are highlighted. 83% of SC neurons (orange) show suppression at 50 ms post-saccade; 68% of tectal neurons (blue) show suppression across the three tested post-saccadic times.

(F) Time course of suppression in monkey SC. Faint lines indicate data from Bellet et al. 2017; crosses show the current data from all neurons (dashed line) and the significantly suppressed ones (solid line), closely matching model predictions. Inset: model prediction for low sensory and motor noise, as in Figure 3A, top left.

(G) Suppression time course for zebrafish tectum neurons, analogous to (F). Inset: model prediction for high sensory and motor noise, as in Figure 3A, bottom right.

In our view, the alignment between modeling and data in our study suggests that efficient sensory-motor estimation under species-specific noise constraints provides a unifying account of saccadic suppression strength across vertebrates. We suggest that theoretical considerations of the implications of computational resource limits, like we did here, will also be valuable for our understanding of a wide range of further multi-modal, integrative brain processes.

Methods

Animal Care

All non-human primate and zebrafish experiments were evaluated by ethics committees and approved by the Tübingen regional government. For macaques we recorded SC activity from two adult, male rhesus macaque monkeys (A and F), aged 13 to 14 y and weighing 9 to 13 kg. For zebrafish we recorded calcium activity larval zebrafish 5-7 days post fertilization (dpf) with pan-neuronal GCaMP6f expression and homozygous for the *mitfa* mutation (*Tg(HuC:H2B-GCaMP6f)jf7; nacre -/-*)[24]. For eye position recordings we used 5-6 dpf larvae *nacre -/-*. Larvae were raised in E3 solution at 28°C on a 14/10 light/dark cycle.

Noise Estimation

Macaque eye position recordings

The eye data used for the noise estimation is a subset of the data published by Soto et al.[25]. It comes from the delayed saccade task, in which the monkey fixated a central spot while a peripheral target (1-degree-diameter circle) appeared and remained visible. After a variable delay (500–1,000 ms), the fixation spot disappeared, cueing a saccade to the target. We used 1,445 trials involving four oblique saccade directions with varying amplitudes. Eye data acquisition and saccade detection were performed similarly to the procedures described below for the current monkeys' task.

Zebrafish eye position recordings

Eye position of larval zebrafish was recorded at 1 kHz with a high-speed camera (iN8-S1 IDT, Integrated Design Tools, Inc., Pasadena, CA, USA) mounted on a stereomicroscope. Spontaneous saccades were detected using a motion trigger and 1000 frames recorded, including 200 frames pre-trigger. Recordings were manually screened for false triggers caused by non-saccadic motion within the frame and, if necessary, discarded. Eye position was extracted post-hoc using the ZebEyeTrack virtual machine[26].

Additive motor noise

Before analysis, zebrafish trials were discarded which did not meet the following criteria: both eyes move along the same direction, saccade amplitude is greater than 5° for both eyes, and traces show no strong fluctuations for either eye. The remaining traces were visually inspected, and 5 further traces clearly showing no saccade were manually discarded. In each trial, saccade onset and offset are detected with a velocity criterion matching the variability of the eye trace[27], and trials split into pre-saccadic, saccadic, and post-saccadic periods accordingly. Additive motor noise is estimated from pre- and post-saccadic data only by fitting one affine function each to the pre- and post-saccadic traces of each trial. Deviations between best fits and raw data are interpreted as noise. We compute them for each time point, pool across trials, then compute their standard deviation to estimate ξ.

Multiplicative motor noise

Multiplicative motor noise is associated with the control signal, and thus estimated from saccadic periods under the assumption that the (previously estimated) additive motor noise remains stationary. We fit a sigmoid function to the saccadic part of each eye trace using a soft ramp[28]. As larvae occasionally show pre-saccadic drift as well as large saccadic overshoots or undershoots, and these are not the object of the present study, such trials are excluded based on fit score. The exclusion threshold is high enough to ensure that both high-noise and low-noise trials with sigmoidal saccades are included, and only significantly distorted saccades excluded. For each trial, we then computed the time derivative of the best fit to estimate control signal u, which is pooled over all eye traces. To facilitate estimation of ε, we convert u into a piecewise-constant function by dividing saccades into time bins of 100 values, computing an average $\bar{u}$ per bin, and discretizing it. Across trials, eye positions with the same discretized $\bar{u}$ are pooled; the standard deviation of their distance from best fits provides one estimate of multiplicative noise per value of $\bar{u}$. As we observed no characteristic differences between estimates obtained under high or low control signals, we averaged them to obtain ε. The arbitrary

scaling parameter α was kept at 0.06 throughout, as this allowed us to reproduce the original model results[5].

Estimation of neuron count within brain areas

Our estimation of sensory noise depended on the difference in number of neurons in primate superior colliculus versus zebrafish optic tectum. The superior colliculus of macaques has an estimated volume of 15 mm^3 (cf. Figure 3D from Chen et al. [29], we used the raw data of the SC surface reconstruction). The average macaque brain has a volume of 90.000 - 100.000 mm^3 and an estimated number of 6 x 10^9 neurons[30,31]. Assuming the neuronal density to be roughly homogeneous, we multiplied the total neuron number by the fraction of SC volume relative to whole brain volume, roughly totaling 10^6 neurons. Note, however, that the homogeneous density assumption is a simplification, since subcortical structures have been reported to have lower neuron density than cortical structures[31]. 7-day-old zebrafish contain about 100,000 neurons[32] and due to the large volume of the OT, we estimate that it contains about 10,000 neurons. Based on our estimated neuron count and assuming, for the sake of argument, a uniform two-dimensional tiling of visual space, the 100-fold difference in neuron count translates into a difference of visual resolution on the order of $\sigma = \sqrt{100} = 10$.

Sensory Estimation Model

To model the effect of noise on efficient sensory estimation, we reconstructed a closed-loop control model that had previously been used to explain the existence and time course of saccadic suppression[5]. This abstract model treats sensory and motor information as simple 4D variables (position and velocity of eye and target, respectively), without any reference to specific neuronal implementations. In addition to our own, the original authors kindly provided unpublished MATLAB code. We manually identified parameters to reproduce the originally published time course and to improve the stability of simulations across a wider range of noise levels. Final parameters (all unitless as per the model) included $\xi \in [0.01, 0.375]$, $\sigma \in [10^{-6}, 10^{-5}]$, scaling factor $\alpha = 0.06$, sensory delay = 0.1, initial fixation time = 0.5, movement time = 0.05, stabilization time = 0.25, cost function tolerance = 0.01, initial target position = -10, final target position = 20, discrete

time step = 0.02. Because inter-species differences were on a comparable order of magnitude in both ξ (37.5x) and ε (10x), and because the effect of multiplicative motor noise ε was relatively minor, we covaried the two types of motor noise in all simulations reported here, with $\varepsilon = \xi$. Because of the model's high degree of abstraction, we cannot directly substitute our experimentally determined noise values. Therefore, we chose an approach, where we first reproduced the curve from the original modeling study[5] and then multiplied the used noise levels to investigate the effects on the saccadic suppression curve (Figure 3).

Macaque Electrophysiology

Experimental setup

The experimental setup closely followed the procedures outlined in our previous study[33]. In brief, experiments were conducted in a darkened room with the animal positioned approximately 72 cm away from a calibrated and gamma-linearized CRT monitor (covering ~30° horizontally and ~23° vertically). Stimulus presentation and data collection were managed using a custom-modified version of PLDAPS[34], integrated with the Psychophysics Toolbox[35] and interfaced with an OmniPlex data acquisition system (Plexon, Inc.).

Animal preparation for behavioral training and electrophysiological recording was carried out as described in earlier work[33]. Briefly, each animal was surgically implanted with a head post for head stabilization and a scleral search coil in one eye[36] to enable high-precision eye tracking via electromagnetic induction[37]. A recording chamber was also implanted along the midline, tilted 38° posterior to vertical to target the superior colliculus. We used linear multi-electrode arrays (V-Probes, Plexon Inc.) with either 20 or 24 channels and 50 µm inter-electrode spacing to record neuronal activity. We minimized sampling bias by offline spike sorting.

Behavioral task

In each trial, monkeys performed a visually guided saccade task against a background of either a fine or a coarse texture. For each texture condition, one of 80 pre-generated images (80 fine, 80 coarse) was randomly selected and displayed as the background.

Each trial began with the presentation of a fixation spot, located 7.56° to the left or right of the screen center. After the monkey acquired and maintained fixation on this spot, it disappeared and simultaneously reappeared at the center of the screen. The monkey was trained to perform a visually guided saccade to the new (central) fixation location and to maintain gaze there for a set duration (500 ms), after which a juice reward was delivered.

During the saccade, when the eye position reached within 2.5° of the new fixation location, a probe flash was triggered. This probe, a square of size 1° × 1°, consisted of a brief luminance change (either an increase or decrease) in the pixel values of the texture at the receptive field (RF) location of the recorded superior colliculus (SC) neurons. The RFs had been previously mapped using a separate task.

The flash could occur at one of three randomly chosen onset times relative to the eye crossing the 2.5° threshold: either immediately (0 ms), or with a delay of 100 ms or 200 ms. Shortly before the initial saccade onset in each trial, we calculated the fixation error and adjusted the probe position accordingly to ensure accurate alignment with the intended RF location.

Data Analysis

Eye position data were recorded at 1 kHz using scleral search coils, and neuronal activity in the superior colliculus (SC) was acquired via laminar probes. Saccades were detected offline using a previously described analysis toolbox[38], and the detected events were manually verified to ensure accuracy.

Spike sorting was performed offline using the Kilosort Toolbox[39], followed by manual refinement with the phy software. Subsequent analyses focused on firing rates across

experimental conditions. Firing rates were estimated by convolving spike trains with a Gaussian kernel (σ = 10 ms).

Only SC neurons that exhibited a significant visual response relative to baseline activity (*t*-test) were included in the analysis. To quantify suppression strength, we employed an analysis approach similar to that used in prior work[9].

First, to isolate the neural response associated with the saccade itself, we aligned spiking activity to the offline-detected saccade onset and averaged responses across the portion of the trial influenced by the saccade but not by the visual probe. This saccade-related response was computed separately for each neuron, saccade direction, and background texture condition.

Next, we aligned the neural activity to the onset of the probe flash and determined the temporal offset between saccade onset and probe onset for each trial. The saccade-related response was then temporally shifted by this offset and subtracted from the individual trial activity, isolating the probe-evoked component of the response.

In this study, we averaged across trials in which the probe flash was either an increase or a decrease in local luminance. Analysis was restricted to trials in which a coarse texture served as the background.

To quantify the degree of suppression, we computed a suppression index for each neuron by dividing the average evoked response in the 0 ms delay condition by the average response in the 200 ms delay condition (baseline). The evoked response was defined as the mean firing rate in the window from 50 to 200 ms after probe onset.

Zebrafish *in-vivo* calcium imaging

Experimental setup

Larval zebrafish were embedded in 1.6% low-melting agarose with the agarose removed around the eyes to allow for free eye movements. The fish were then placed onto a custom-built stage and submerged in E3 within a spherical stimulation arena, previously

described[11]. Visual stimuli were projected onto the surface of the stimulation arena at 60 Hz refresh rate at 625 nm.

To measure eye position, the fish were illuminated using a custom-built IR-LED ring and the eyes were recorded with an infrared-filtered camera (Basler ace 2 R, a2A1920-160umBAS, Basler AG, Ahrensburg, Germany) at 100 Hz. Fish were allowed to perform spontaneous saccades. Eye position was extracted online and instantaneous velocity computed. Saccades were detected, using a velocity threshold of at least 200°/s. To optimize saccade detection, the actual velocity threshold was adjusted for each fish to ensure ideal saccade detection and to avoid noise interference. To generate and display visual stimuli, to extract eye position and velocity and to trigger visual stimuli in a closed-loop manner we used *VxPy* (Version 0.1.4).

To measure calcium activity in tectal neurons we used a moveable objective two-photon setup (Sutter Instruments, Novato, CA, USA) with an acquisition rate of 2.18 fps, an image size of 512 x 512 pixels and a resolution of 0.88 µm x 0.88 µm per pixel. GCaMP6f was excited at 920 nm and emitted light was collected using a 20x/1.0 Zeiss water immersion objective.

Visual stimuli

Binary gaussian blur textures were displayed onto the spherical stimulation arena, as previously described[11]. In response to spontaneous saccades after a delay period of 20, 100, 250, 500, 1000, 2000, or 4000 ms a probe flash consisting of a whole-field luminance decrease with a cosine shape, lasting 500 ms at 0.5 Hz and an amplitude of 50% luminance change was displayed. To obtain a baseline response to the probe flash, it was also shown 8 s after saccade detection to ensure no temporal connection between saccade and probe flash.

Data Analysis

Calcium recordings were registered and segmented into ROIs using suite2p[40]. Further analysis of registered ROIs was performed with custom-written Python (PyCharm, JetBrains, Prague, Czech Republic) and Matlab (The MathWorks Inc., Natick, USA) code.

Fluorescence traces of individual ROIs were normalized to $\Delta F/F_0$, where F_0 was a 120 second sliding median window. ROIs that showed responses to the probe flash were identified using regression-based analysis and only those ROIs were considered for further analysis. For each ROI, saccade related responses were quantified, using control conditions, where no probe flash was shown. Said saccade-related response was subtracted in all other conditions during and shortly after the time of the saccade. Peak $\Delta F/F_0$ responses to probe flashes were quantified and averaged for each delay condition. For each ROI a suppression index for each delay was computed as in the macaque data. Amongst all probe flash-responsive ROIs, truly suppressed ROIs were identified with a permutation test, described previously[11].

References

1. Wurtz, R. H. Neuronal mechanisms of visual stability. *Vision Res* **48**, 2070–2089 (2008).
2. Sommer, M. A. & Wurtz, R. H. Brain circuits for the internal monitoring of movements. *Annu Rev Neurosci* **31**, 317 (2008).
3. Zuber, B. L. & Stark, L. Saccadic suppression: Elevation of visual threshold associated with saccadic eye movements. *Exp Neurol* **16**, 65–79 (1966).
4. Beeler, G. W. Visual threshold changes resulting from spontaneous saccadic eye movements. *Vision Res* **7**, 769–775 (1967).
5. Crevecoeur, F. & Kording, K. P. Saccadic suppression as a perceptual consequence of efficient sensorimotor estimation. *Elife* **6**, (2017).
6. Bremmer, F., Kubischik, M., Hoffmann, K. P. & Krekelberg, B. Neural dynamics of saccadic suppression. *Journal of Neuroscience* **29**, 12374–12383 (2009).
7. Hafed, Z. M. & Krauzlis, R. J. Microsaccadic suppression of visual bursts in the primate superior colliculus. *Journal of Neuroscience* **30**, 9542–9547 (2010).
8. Burr, D. C., Morrone, M. C. & Ross, J. Selective suppression of the magnocellular visual pathway during saccadic eye movements. *Nature 1994 371:6497* **371**, 511–513 (1994).
9. Idrees, S., Baumann, M. P., Franke, F., Münch, T. A. & Hafed, Z. M. Perceptual saccadic suppression starts in the retina. *Nat Commun* **11**, 1–19 (2020).
10. Idrees, S. *et al.* Suppression without inhibition: how retinal computation contributes to saccadic suppression. *Communications Biology 2022 5:1* **5**, 1–23 (2022).
11. Soto, G. *et al.* Saccadic Suppression Enhances Saliency of Prey-Like Stimuli in the Optic Tectum. *bioRxiv* 2025.02.21.639462 (2025) doi:10.1101/2025.02.21.639462.
12. Jing Chen, X., Valsecchi, M. & Gegenfurtner, K. R. Saccadic suppression measured by steady-state visual evoked potentials. *J Neurophysiol* **122**, 251–258 (2019).
13. Zhang, Y., Valsecchi, M., Gegenfurtner, K. R. & Chen, J. The execution of saccadic eye movements suppresses visual processing of both color and luminance in the early visual cortex of humans. *J Neurophysiol* (2024) doi:10.1152/JN.00419.2023.
14. Liu, X. *et al.* The Superior Colliculus: Cell Types, Connectivity, and Behavior. *Neurosci Bull* **38**, 1519 (2022).
15. Cang, J., Savier, E., Barchini, J. & Liu, X. Visual function, organization, and development of the mouse superior colliculus. *Annu Rev Vis Sci* **4**, 239–262 (2018).

16. Chen, C. Y. & Hafed, Z. M. A neural locus for spatial-frequency specific saccadic suppression in visual-motor neurons of the primate superior colliculus. *J Neurophysiol* **117**, 1657–1673 (2017).
17. Wurtz, R. H. & Albano, J. E. Visual-motor function of the primate superior colliculus. *Annu Rev Neurosci* **3**, 189–226 (1980).
18. Isa, T., Marquez-Legorreta, E., Grillner, S. & Scott, E. K. The tectum/superior colliculus as the vertebrate solution for spatial sensory integration and action. *Current Biology* **31**, R741–R762 (2021).
19. Chen, C. Y., Ignashchenkova, A., Thier, P. & Hafed, Z. M. Neuronal response gain enhancement prior to microsaccades. *Current Biology* **25**, 2065–2074 (2015).
20. Wu, W. & Hafed, Z. M. Stronger premicrosaccadic sensitivity enhancement for dark contrasts in the primate superior colliculus. *Scientific Reports 2025 15:1* **15**, 1–17 (2025).
21. Easter, S. S. & Nicola, G. N. The development of vision in the zebrafish (Danio rerio). *Dev Biol* **180**, 646–663 (1996).
22. Rolls, E. T. & Cowey, A. Topography of the retina and striate cortex and its relationship to visual acuity in rhesus monkeys and squirrel monkeys. *Exp Brain Res* **10**, 298–310 (1970).
23. Schwartz, E. L. Spatial mapping in the primate sensory projection: Analytic structure and relevance to perception. *Biol Cybern* **25**, 181–194 (1977).
24. Dunn, T. W. *et al.* Brain-wide mapping of neural activity controlling zebrafish exploratory locomotion. *Elife* **5**, (2016).
25. Hafed, Z. M. & Chen, C. Y. Sharper, Stronger, Faster Upper Visual Field Representation in Primate Superior Colliculus. *Current Biology* **26**, 1647–1658 (2016).
26. Dehmelt, F. A., Von Daranyi, A., Leyden, C. & Arrenberg, A. B. Evoking and tracking zebrafish eye movement in multiple larvae with ZebEyeTrack. *Nat Protoc* **13**, 1539–1568 (2018).
27. Nyström, M. & Holmqvist, K. An adaptive algorithm for fixation, saccade, and glissade detection in eyetracking data. *Behav Res Methods* **42**, 188–204 (2010).
28. Dai, W., Selesnick, I., Rizzo, J. R., Rucker, J. & Hudson, T. A parametric model for saccadic eye movement. *2016 IEEE Signal Processing in Medicine and Biology Symposium, SPMB 2016 - Proceedings* (2017) doi:10.1109/SPMB.2016.7846860.
29. Chen, C. Y., Hoffmann, K. P., Distler, C. & Hafed, Z. M. The Foveal Visual Representation of the Primate Superior Colliculus. *Current Biology* **29**, 2109-2119.e7 (2019).

30. Scott, J. A. *et al.* Longitudinal analysis of the developing rhesus monkey brain using magnetic resonance imaging: birth to adulthood. *Brain Struct Funct* **221**, 2847–2871 (2016).
31. Herculano-Houzel, S., Collins, C. E., Wong, P. & Kaas, J. H. Cellular scaling rules for primate brains. *Proc Natl Acad Sci U S A* **104**, 3562–3567 (2007).
32. Sumbre, G. & de Polavieja, G. G. The world according to zebrafish: how neural circuits generate behavior. *Front Neural Circuits* **8**, 91 (2014).
33. Bogadhi, A. R. & Hafed, Z. M. Express detection of visual objects by primate superior colliculus neurons. *Sci Rep* **13**, 1–15 (2023).
34. Eastman, K. M., Huk, A. C. & Galloway, G. J. PLDAPS: A Hardware Architecture and Software Toolbox for Neurophysiology Requiring Complex Visual Stimuli and Online Behavioral Control. *Front Neuroinform* **6**, 14243 (2012).
35. Brainard, D. H. The Psychophysics Toolbox. *Spat Vis* **10**, 433–436 (1997).
36. Judge, S. J., Richmond, B. J. & Chu, F. C. Implantation of magnetic search coils for measurement of eye position: An improved method. *Vision Res* **20**, 535–538 (1980).
37. Fuchs, A. F. & Robinson, D. A. A method for measuring horizontal and vertical eye movement chronically in the monkey. *J Appl Physiol* **21**, 1068–1070 (1966).
38. Chen, C. Y. & Hafed, Z. M. Postmicrosaccadic Enhancement of Slow Eye Movements. *Journal of Neuroscience* **33**, 5375–5386 (2013).
39. Pachitariu, M., Steinmetz, N. A., Kadir, S. N., Carandini, M. & Harris, K. D. Fast and accurate spike sorting of high-channel count probes with KiloSort. *Adv Neural Inf Process Syst* **29**, (2016).
40. Pachitariu, M. *et al.* Suite2p: beyond 10,000 neurons with standard two-photon microscopy. *bioRxiv* 061507 (2017) doi:10.1101/061507.

Acknowledgements

This work was funded by the Deutsche Forschungsgemeinschaft (DFG; German Research Foundation) through the Special Priority Programme: “SPP 2205 Evolutionary optimization of neural processing” (430158665; AR 1076/1-2, HA 6749/3-2, AR 1076/1-1), by the Major Research Instrumentation programme of the DFG (INST 37/1254-1 FUGG), and by the Human Frontier Science Program (HFSP) Young Investigator grant RGY0079. We're grateful to Frédéric Crèvecoeur of UC Louvain, Belgium, for sharing code and advice on how to approximate their original model results.

Author Contributions

G.S. performed experiments in zebrafish optic tectum, analyzed zebrafish calcium data, generated figures, and wrote the manuscript. F.A.D. reproduced the saccadic suppression model, generated figures, and wrote the manuscript. M.P.B. performed macaque experiments, analyzed macaque eye movement data, analyzed macaque electrophysiology data, generated figures, and wrote the manuscript. I.T. analyzed zebrafish and macaque eye trace data and generated figures. Y.Y. performed macaque experiments. T.M. performed macaque experiments and analyzed macaque electrophysiology data. Z.M.H. and A.B.A. designed the overall study, acquired funding and wrote the manuscript.

Competing Interests

The authors declare no competing interests.